ISJ 23: 1-9, 2026 ISSN 1824-307X

RESEARCH REPORT

# Differential expression of pathogenic factors *pirA* and *pirB* from *Vibrio parahaemolyticus* causing acute hepatopancreatic necrosis disease at nucleic acid and protein levels: implications for pathogen detection

**S-R Shao[1,2], H-R Yang[1,2], M-Q Wang[1,2,3,4*]**

*[1]MOE Key Laboratory of Marine Genetics and Breeding, Shandong Key Laboratory of Marine Seed Industry (preparatory), Ocean University of China, Qingdao 266003, China*
*[2]Hainan Key Laboratory of Tropical Aquatic Germplasm (Hainan Seed Industry Laboratory), Sanya Oceanographic Institution, Ocean University of China, Sanya 572024, China*
*[3]Hebei Xinhai Aquatic Biotechnology Company Limited, Cangzhou 061100, China*
*[4]Hainan Lanyin Aquatic Breeding Technology Company Limited, Wenchang 571343, China*

 *Accepted February 5, 2026*

## Abstract

*Litopenaeus vannamei* is one of the most economically valuable aquaculture species. In recent years, the shrimp industry has experienced considerable economic losses due to various diseases such as acute hepatopancreatic necrosis disease (AHPND). AHPND is a disease caused by certain strain of *Vibrio parahaemolyticus* carrying a specific plasmid pVA1. The pVA1 plasmid contains the *pirA* and *pirB* genes, which encode the main virulence factors of AHPND. In light of the dearth of effective treatment options, the development of expeditious, precise, and effective methodologies for detecting AHPND pathogens is imperative to prevent the onset of disease in shrimp farming. However, current nucleic acid based and antibody-based detection methods sometimes produce false positive results, affecting the reliability of diagnosis. This study aims to make a comparison of the content of the *pirA* and *pirB* virulence factors at the DNA, RNA, and protein levels in order to investigate whether there is a corresponding relationship between the pathogenic factors of AHPND at the nucleic acid and protein levels, which will provide a foundation for the selection of pathogen detection methods for shrimp. At the mRNA level, the expression level of *pirA* is significantly higher than that of *pirB*. Conversely, at the protein level, the expression level of PirB protein is much higher than that of PirA protein, indicating that the results of the two different detection methods are contradictory. Therefore, relying solely on nucleic acid or protein testing may not accurately assess whether shrimp are diseased. In the future, a combined nucleic acid and protein testing strategy could be implemented to enhance diagnostic accuracy and ensure the sustainable development of the shrimp farming industry.

**Key Words**: *Litopenaeus vannamei*; *Vibrio parahaemolyticus*; acute hepatopancreatic necrosis disease

## Introduction

*Litopenaeus vannamei* is one of the most economically valuable species in aquaculture. However, during the process of cultivation, inadequate management and other factors frequently result in the proliferation of numerous diseases. Acute hepatopancreatic necrosis disease (AHPND), has inflicted substantial economic losses on the *L. vannamei* industry owing to its rapid transmission and high mortality rates (Li *et al*., 2019). *Vibrio parahaemolyticus* has been identified as a primary pathogen that causes AHPND in shrimp. It is a gram-negative halophilic bacterium that carries the pVA1 plasmid, which contains the genes encoding the binary toxins *pirA* and *pirB* (Lee *et al*., 2015). It has been established that these two toxins represent the core virulence factors of AHPND, exhibiting functional characteristics analogous to those of the Cry protein in *Bacillus thuringiensis*. They form a binary complex that has been demonstrated to cause damage to the hepatopancreatic tissue of shrimp (Han *et al*., 2015). Currently, no efficacious treatment methods for shrimp infected with AHPND were available, so early detection represents a critical strategy for preventing further propagation of the disease.

*Corresponding author:*
Mengqiang Wang
MOE Key Laboratory of Marine Genetics and Breeding
Shandong Key Laboratory of Marine Seed Industry (preparatory)
Ocean University of China
Qingdao 266003, China
E-mail: wangmengqiang@ouc.edu.cn

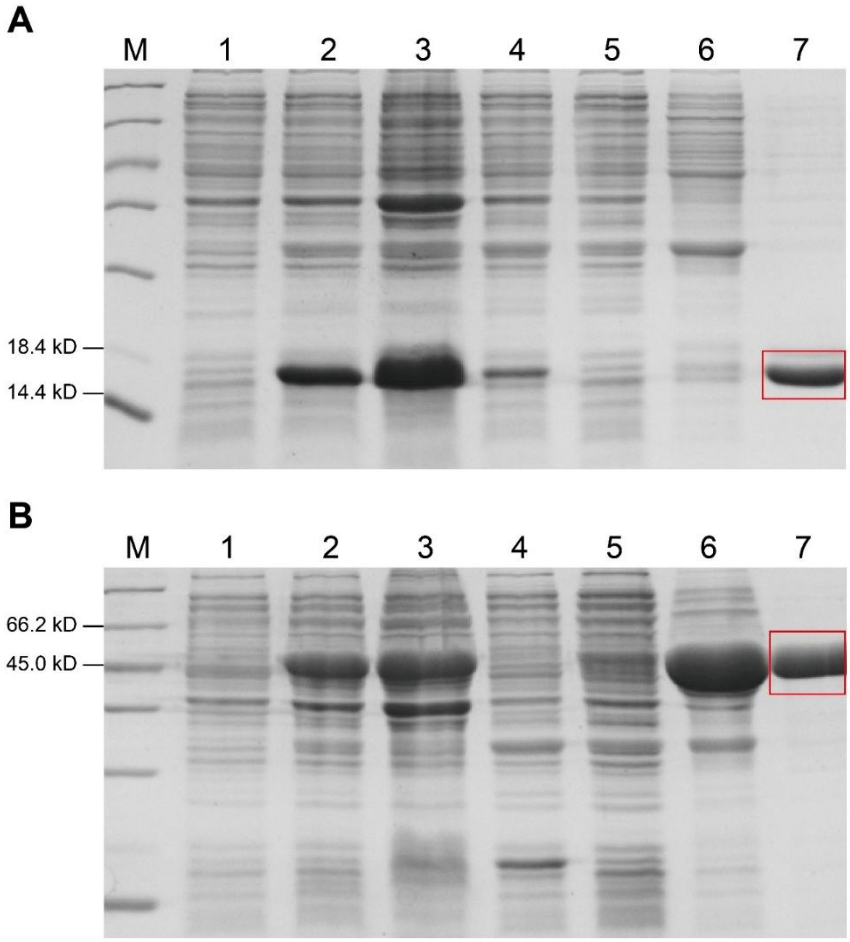


**Fig. 1** SDS-PAGE analysis of purified recombinant proteins PirA and PirB. Lane M: Protein molecular weight standard; Lane 1: the total proteins of *E. coli* with PirA or PirB, without IPTG induction; Lane 2: the total protein of *E. coli* with PirA or PirB, induction with IPTG; Lane 3: the mixture of IPTG-induced bacterial cells broken by ultrasonication; Lane 4: Supernatant after ultrasonication and centrifugation; Lane 5: the fluid flows through the Ni-NTA columns; Lane 6: the impurity proteins washed away by low-concentration imidazole; Lane 7: purified PirA or PirB by Ni-NTA chromatography

At present, the primary detection methods for AHPND include nucleic acid-based testing and antibody-based one, both of which primarily target the virulence factors *pirA* and *pirB*. For instance, a number of molecular diagnostic methods primarily rely on PCR, including conventional PCR (Sirikharin *et al*., 2015), nested PCR (Dangtip *et al*., 2015), quantitative real-time PCR (qPCR) (Han *et al*., 2015). Other methods include loop-mediated isothermal amplification (LAMP) (Kongrueng *et al*., 2015), real-time enzymatic recombinase amplification (RT-ERA) (Zhou *et al*., 2023), and RPA-CRISPR/Cas12a based on lateral flow strips (Li *et al*., 2022). Despite the fact that these methodologies demonstrate elevated specificity and sensitivity in the identification of AHPND, they are costly and operationally complex. However, it has been observed that certain strains are found to carry the *pirA* and *pirB* genes yet do not produce toxins, consequently resulting in the absence of disease symptoms. This phenomenon can lead to the production of false-positive results through PCR based methods (Phiwsaiya *et al*., 2017; Vicente *et al*., 2020). Furthermore, antibody-based diagnostic methods in protein level are more convenient than molecular diagnostic methods but lack sensitivity (Mai *et al*., 2020; Duong *et al*., 2022; Duong *et al*., 2023; Shao *et al*., 2025). Previous established detection methods for AHPND have all relied on the presence of the *pirA* and *pirB* virulence factors. Nevertheless, these methods exclusively examine individual attributes of molecules or proteins while neglecting to investigate the interconnection between these two states. Consequently, we hypothesize that detection based on a solitary attribute may possess an inherent lack of precision. Therefore, this study aims to make a comparison of the content of the *pirA* and *pirB* virulence factors in different states in order to investigate whether there is a corresponding relationship between the pathogenic factors of AHPND at the nucleic acid and protein levels, which will provide a theoretical basis for the detection of shrimp pathogens.

## Materials and Methods

*Preparation of antigens of PirA and PirB and standard recombinant plasmid*

The antigens of PirA and PirB utilized in this experiment were retrieved from our laboratory and prepared according to the protocol that had been established in a previous study (Shao *et al*., 2025). In brief, the pirA and pirB gene fragments were amplified and cloned into the pEASY-Blunt E1 vector, followed by transformation into *Escherichia coli* BL21 (DE3). Protein expression was induced by 1 mM IPTG and incubated at 37 °C for 4 hours, and it was then purified using a Ni-NTA affinity chromatography system. The standard recombinant plasmids containing *pirA* and *pirB* genes used in this experiment were prepared as previously described (Zhou *et al*., 2023), and subsequently employed for absolute quantification experiments. Other bacterial samples were obtained from our laboratory.

*Growth curve measurement and samples collection of* V. parahaemolyticus

The *V. parahaemolyticus* strain E1 used in this experiment was provided by Prof. Lei Wang, Institute of Oceanography, Chinese Academy of Sciences. Firstly, 5 μL of the bacterial glycerol stock was inoculated onto LB agar plates containing 2% NaCl and streaked for isolation, the plates were then incubated at 28 °C overnight to activate the strains. A single colony was selected and transferred into 5 mL of 2216E liquid medium (HB0132-1, Hopebiol, China), followed by overnight incubation. Subsequently, the overnight culture was further transferred into 400 mL of 2216E medium at a ratio of 1:1000 and incubated under the same conditions. The $OD_{600}$ of the bacterial solution was monitored hourly over a 12-hour period. Concurrently, samples were collected at each time point for subsequent extraction of DNA, RNA and protein. All samples were processed within one week of storage.

*Extraction of total bacterial protein*

Total proteins of *V. parahaemolyticus* were exacted using Bacterial Protein Extraction Kit (C600596, Sangon, China). Samples were collected at 0, 2, 4, 6, 8, 10 and 12 hours, with each time point involving the collection of 2 mL of bacterial sample and the resuspension of the bacterial precipitate in 400 μL of 1× Cell Lysis Buffer per 2 mL of bacterial culture. Subsequent steps were completed according to the manufacturer's protocol, and the final protein extract was collected into a sterile tube for subsequent experiments.

*Dot Blot*

In the Dot Blot experiments, the PirA and PirB antigens were used as standards to establish a standard curve. The purified recombinant proteins were diluted in six distinct concentration gradients (2.5, 5, 7.5, 10, 12.5, 15 ng/μL) and 2 μL of each dilution was added dropwise to the nitrocellulose membrane, obtaining six dots with protein contents of 5, 10, 15, 20, 25, and 30 ng in sequence. The PirA and PirB proteins were added to two different NC membranes, designated as membrane A and membrane B. Then, 2 μL of the total bacterial protein extracted in the preceding step at 0, 2, 4, 6, 8, 10 and 12 hours was added dropwise to each of the two membranes. After drying the membrane at 37 °C for 30 minutes, 5% skimmed milk-TBST was used to block for 1 hour. Subsequently, membrane A and B were incubated respectively with customized anti-PirA/PirB rabbit polyclonal antibody (Abclonal, China) at a final concentration of 0.1 ng/μL as primary antibodies for 1 hour. After washed 6 times by TBST, the HRP-labeled Goat Anti-Rabbit IgG (H+L) antibody (A0208, Beyotime, China) was added as secondary antibody and incubated for 1 hour. Following the washing step, the membranes were incubated in ECL solution (SQ201, Epizyme, China) for one minute. Finally, the visualization results were obtained using a UVP Glestudio plus imaging system (Analytikjena, Germany), the points were analyzed in greyscale using Image J software, and the data were analyzed and illustrated using GraphPad Prism 8.0.1.

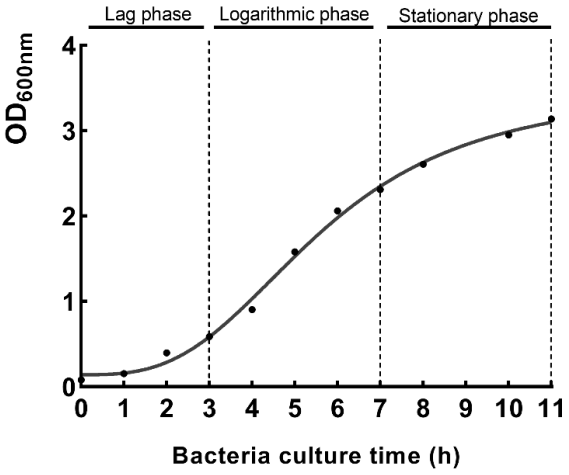


**Fig. 2** Growth curve of *V. parahaemolyticus*. Cultivate *V. parahaemolyticus* strains and record $OD_{600}$ once per hour until 11 hours after inoculation. There are three periods: lag phase, logarithmic phase, and stationary phase

*Collection of experimental diseased shrimp*

Six shrimps infected with AHPND were arbitrarily chosen from a shrimp farm in Dongfang City, China. The samples used in this study were obtained from artificially infected experiments and the AHPND infection was confirmed through observation of clinical symptoms, mortality rates, and PCR detection of the *pirA* and *pirB* genes. The hepatopancreas of the diseased shrimp was collected for subsequent detecting and comparison of the content of *pirA* and *pirB*.

*DNA extraction*

The total DNA of *V. parahaemolyticus* cultured for 0-11 hours was extracted respectively using the TIANamp Bacteria DNA Kit (DP302, Tiangen, China). Then, the total DNA from the hepatopancreas of each of the six diseased shrimps with AHPND was extracted using the TIANamp Marine Animals DNA Kit (DP324, Tiangen, China). The extracts were then stored at -20 °C for subsequent use.

*Total RNA extraction and cDNA synthesis*

The total RNA extraction of *V. parahaemolyticus* in this experiment was performed using a Bacteria Total RNA Isolation Kit (B518625, Sangon, China). Briefly, 1 mL of bacteria that had been cultured for 0-11 hours was subjected to centrifugation in order to remove the medium. Subsequently, 100 μL of lysozyme (RT401, Tiangen, China) at a concentration of 400 μg/ml was incorporated, and digested for 5 minutes. The subsequent steps were completed in accordance with the instructions of the kit, thereby yielding the total RNA of *V. parahaemolyticus*. The total RNA from the hepatopancreas of six diseased shrimps with AHPND was extracted using TRIzol Reagent (15596026, Invitrogen, USA). The experiment was conducted in accordance with the manufacturer's manual. The synthesis of cDNA was conducted using the HiScript III 1st Strand cDNA Synthesis Kit (+gDNA wiper) (R312-02, Vazyme, China), following the manufacturer's instructions. Ultimately, the cDNA was stored at -20 °C for the subsequent expression analysis experiments.

*Quantitative real-time PCR analysis*

Quantitative real-time PCR (qPCR) was used to analyze and compare the DNA content and mRNA expression levels of *pirA* and *pirB* genes in different samples. First, the copy number of the recombinant standard plasmid was calculated using the following formula:

$$\text{Copy number (copies/μL)} = \frac{\text{concentration(ng/μL)} \times 10^{-9} \times 6.022 \times 10^{23}\ \text{(copies/mol)}}{\text{clone size(bp)} \times 660\text{(g/mol/bp)}}$$

Thereafter, gradient dilutions were executed, ranging from $10^7$ to $10^2$ copies/μL. Subsequently, gradient dilution of the standard plasmids was employed as templates for qPCR amplification targeting the pathogenic *pirA* and *pirB* genes. The qPCR reaction was conducted in a final volume of 20 μL within a system composed of 10 μL of 2 × ChamQ Universal SYBR qPCR premix (Q711, Vazyme, China), 8.2 μL of dd$H_2O$, 0.4 μL of 10 μM forward primer *VppirA*-F (5'-TTGGACTGTCGAACCAAACG-3') or *VppirB*-F (5'-GTTTCACCGATTCTGATGTGC-3'), 0.4 μL of 10 μM reverse primer *VppirA*-R (5'-GCACCCCATTGGTATTGAATG-3') or *VppirB*-R (5'-GTAAGAGTCGTTATCAGCCCAC-3'), and 1 μL of serially diluted standard plasmid template ($10^2$-$10^7$ copies/μL). The real-time PCR primers were designed based on the published nucleotide sequences of the target genes retrieved from the NCBI GenBank database. Specifically, the *pirA* gene sequence (GenBank accession number KM067908.1, positions 17198-17533) and *pirB* gene sequence (GenBank accession number KM067908.1, positions 17546-18862) were utilized in this study. Primer design was then performed using the Primer Premier 5 software to generate amplicons suitable for quantitative PCR. The copy number of the standard plasmid in the experiment was designated as the x-axis, and the Cq values of *pirA* or *pirB* genes at varying copy number were designated as the y-axis. The standard curve was plotted to obtain the linear regression equation. Subsequently, qPCR experiments were conducted according to the above experimental steps using the DNA and cDNA from *V. parahaemolyticus* cultured for different times and the DNA and cDNA from the hepatopancreas of six diseased shrimps with AHPND as templates according to the above system. The experimental results were subsequently substituted into the linear regression equations of *pirA* or *pirB* genes, respectively, to compared the DNA content and mRNA expression levels of *pirA* and *pirB* genes in diverse samples through absolute quantification.

**Results**

*Expression and purification of recombinant PirA and PirB proteins*

Based on previous findings, PirA and PirB proteins are expressed in the pEASY-Blunt Zero system. Whole-cell lysates of *E. coli* BL21 (DE3) cells induced with IPTG were subsequently analyzed using SDS-PAGE gels (Fig. 1). Compared to non-induced cells (Fig. 1, lane 1), a distinct band with a molecular weight of approximately 13 kDa (PirA, Fig. 1A, lane 2) and 52 kDa (PirB, Fig. 1B, lane 2) were observed. SDS-PAGE analysis demonstrated the effective removal of impurity proteins, and a significant amount of relatively pure PirA or PirB protein was obtained in the eluate fraction analyzed (Fig. 1, lane 7).

*Construction of bacterial growth curves*

The growth curve of *V. parahaemolyticus* was recorded to ascertain the growth time of the bacterium to each stage of growth (Fig. 2). Initially, the lag phase persisted for approximately 3 hours ($OD_{600}$ from 0.01 to 0.6), the logarithmic phase continued until the 7th hour ($OD_{600}$ from 0.6 to 2.2), and the stationary phase is the 8-11th hours ($OD_{600}$ from 2.2 to 3.2). Therefore, the bacterial samples that were incubated for 0-11 hours were selected for subsequent experiments, respectively.

*The content of PirA and PirB proteins in different growth phages of* V. parahaemolyticus

The PirA or PirB recombinant protein standards (5, 10, 15, 20, 25, 30 ng) was used as the x-axis, and the corresponding grey value of each point was used as the y-axis to plot the standard curve and obtain the linear regression equation (Fig. 3A and 3B). Subsequently, the grey values of bacterial proteins at each time point (0, 2, 4, 6, 8, 10, 12 h) were substituted into the equation to obtain the contents of PirA and PirB in bacterial proteins at each time point (Fig. 3C). The experimental results demonstrated that the contents of PirA and PirB in the bacterial proteins were undetectable at 0 h and 2 h owing to the low bacterial concentration. The content of PirB in bacterial proteins was significantly higher than PirA in the later time periods.

*Construction of nucleic acid standard curves*

The nucleic acid analyzer indicated that the concentration of the prepared plasmid standard was 415 ng/μL. The copy number of the plasmid standard was calculated by entering the concentration of plasmid standard and the number of bases into the formula, resulting in 6.5 × $10^{10}$ copies/μL. Following

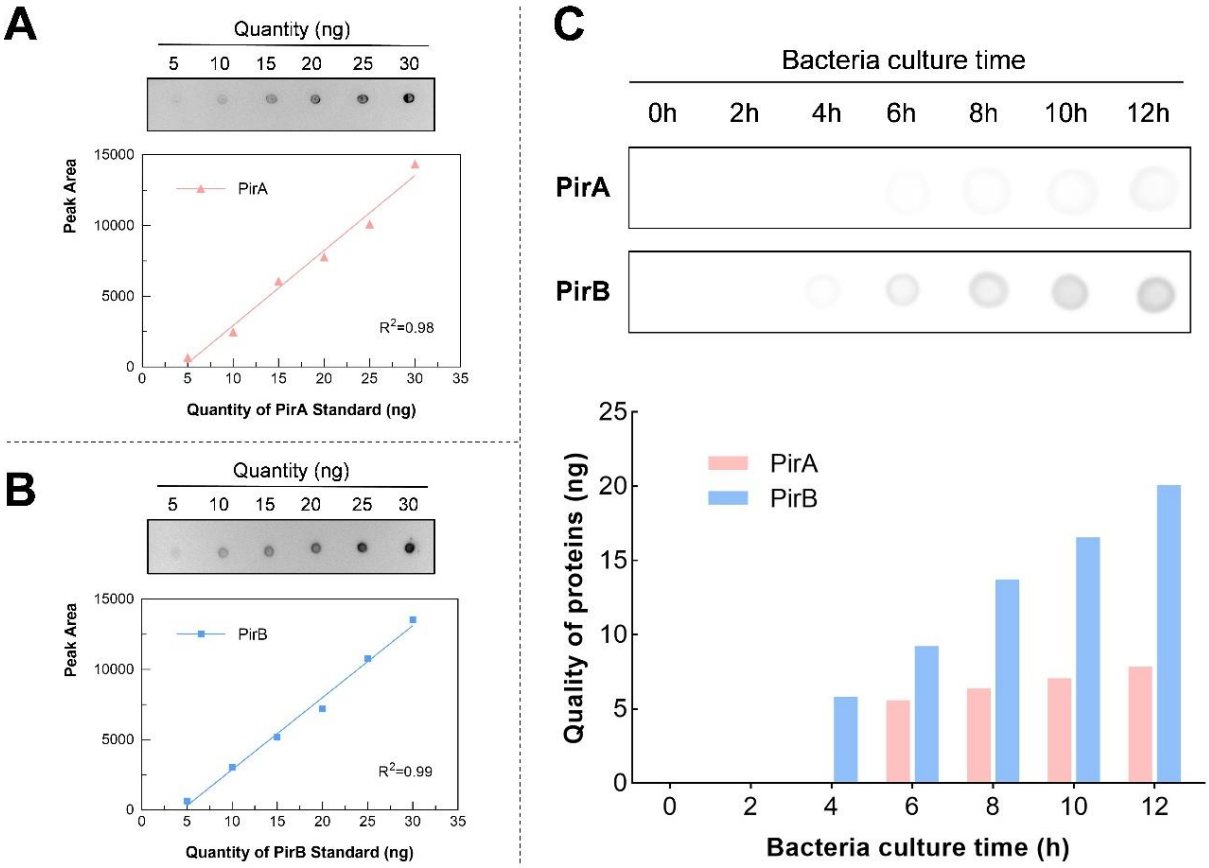


**Fig. 3** Comparison of protein expression levels of PirA and PirB in *V. parahaemolyticus* at different growth stages by Dot Blot. (A) The Dot Blot standard curve of the PirA recombinant protein standard, (B) the Dot Blot standard curve of the PirB recombinant protein standard, (C) the total protein from *V. parahaemolyticus* was extracted at different time points and transferred to two NC membranes (2 μL each point). The membranes were then incubated with antibodies specific to PirA and PirB, respectively. The color development results are shown in the figure

serial 10-fold dilution, six suitable copy number gradients were selected as qPCR templates to obtain the amplification curves (Fig. 4A and 4C). The standard curve was plotted, with the logarithm of the copy numbers serving as the horizontal coordinate and the Cq value as the vertical coordinate (Fig. 4B and 4D). The linear regression equation was obtained and labelled on the graph. The efficiencies for VppirA-F/R and VppirB-F/R were 97.2% and 94.1%, respectively, with correlation coefficients ($R^2$) above 0.99. These results indicated that the standard curve was highly reliable, demonstrating a good linear relationship between the logarithm of the copy number concentration of the plasmid standard and the Cq value.

*DNA content and mRNA expression levels of* pirA *and* pirB *in different growth phases of* V. parahaemolyticus

In the present study, qPCR experiments were conducted using the DNA or cDNA from *V. parahaemolyticus* at varying growth stages as templates in order to obtain the corresponding Cq values. Subsequently, these values were entered into the linear regression equation of the nucleic acid standard curve to calculate the corresponding copy numbers for each sample (Fig. 5). It was found that the DNA content of *pirA* and *pirB* exhibited an initial low level at hour 0-1 due to the low concentration of the bacterial solution. Thereafter, there was a rapid increase at hour 1-2, subsequently stabilizing at a high level. A comparison of the DNA content of *pirA* and *pirB* revealed that both genes exhibited consistent levels throughout the experiment, with *pirA* demonstrating a slightly higher DNA content compared to *pirB* (Fig. 5A). As for the expression levels of mRNA, *pirA* and *pirB* remained at low levels before entering the logarithmic phase. The expression levels reached a maximum at hour 4, subsequently declining from hour 5 and maintaining at a consistently low level. The trends in mRNA expression levels of *pirA* and *pirB* exhibited consistency across all growth stages. However, in general, the mRNA expression levels of *pirA* were found to be obviously higher than those of *pirB* (Fig. 5B).

*DNA content and mRNA expression levels of* pirA *and* pirB *in shrimp infected with AHPND*

The qPCR experiments were conducted utilizing the DNA and cDNA extracted from the hepatopancreas of six randomly selected AHPND-

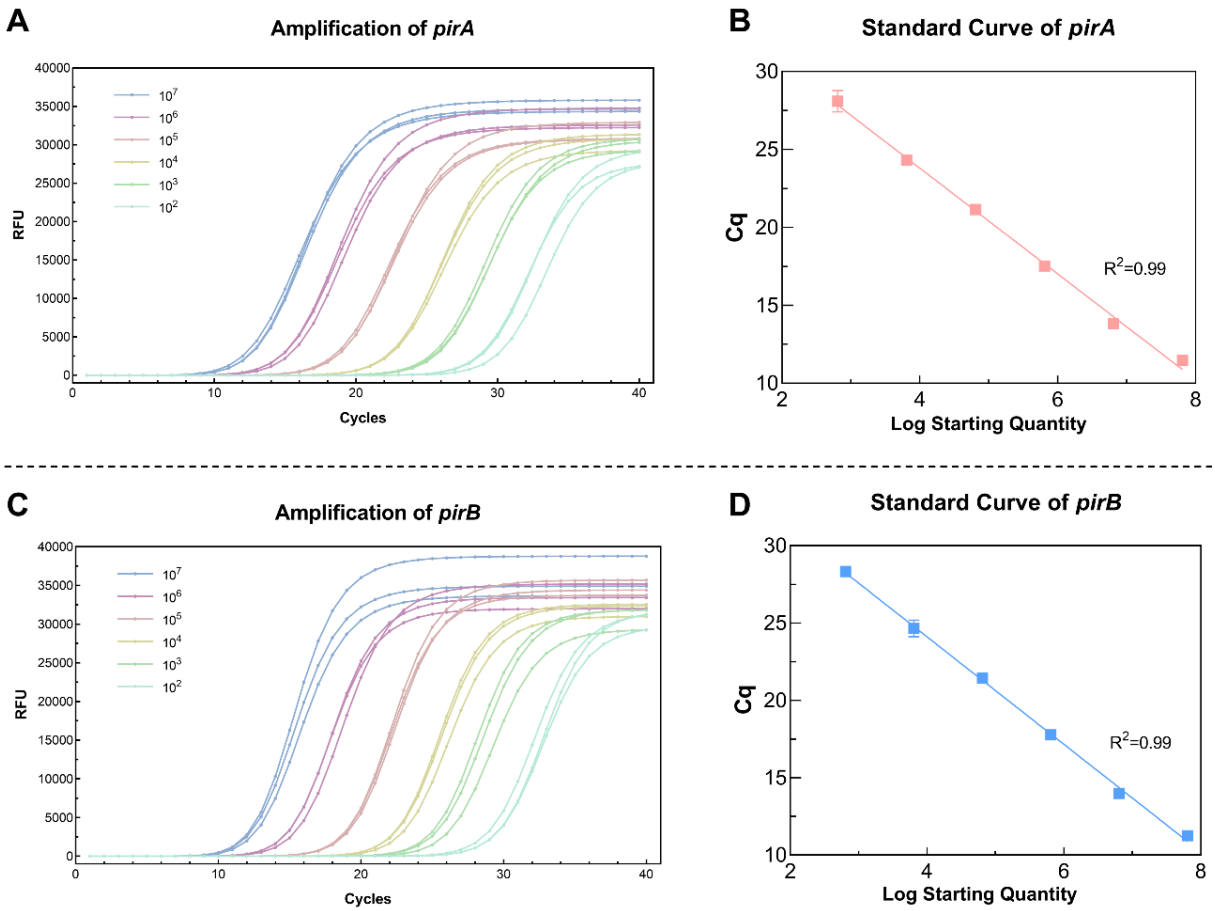


**Fig. 4** Construction of nucleic acid standard curves using standard plasmids containing the *pirA* and *pirB* genes by qPCR. (A) Amplification curve and standard curve of the *pirA* gene. (B) Amplification curve and standard curve of the *pirB* gene. Error bars represent the mean ± SD (n = 3)

affected shrimp as templates (Fig. 6). The results revealed that the DNA content of *pirA* and *pirB* remained consistent over time, with the DNA content of *pirA* being slightly higher than that of *pirB* (Fig. 6A). With regard to the level of mRNA expression, *pirA* was found to be expressed at a higher level than *pirB* in all six diseased shrimp (Fig. 6B). This result is consistent with the experimental results observed in *V. parahaemolyticus* at varying growth stages.

## Discussion

The pathogenic bacteria of AHPND, *V. parahaemolyticus*, carries a pVA1 plasmid containing the binary toxin *pirA* and *pirB* genes, which encode the primary virulence factors of AHPND (Han *et al*., 2015). At present, the primary detection methods for AHPND consist of nucleic acid based and antibody-based approaches. This study adopts both approaches simultaneously, examining the expression tendencies of *pirA* and *pirB* in *V. parahaemolyticus* at the DNA, RNA, and protein levels, and laying a theoretical foundation for the selection of disease diagnosis.

Utilizing total DNA from hourly samples during bacterial growth as a template for qPCR, it was determined that the results for *pirA* and *pirB* were almost identical, indicating that the copy numbers of *pirA* and *pirB* are equivalent in the plasmid carried by *V. parahaemolyticus*. Moreover, these results imply that the copy number of the pVA1 plasmid remains relatively stable, with no loss or amplification occurring. Subsequently, cDNA obtained from reverse transcription of total RNA was used as a template to observe and compare the mRNA expression levels of *pirA* and *pirB* at different stages of bacterial growth. Research had demonstrated that the mRNA expression levels of *pirA* and *pirB* remained at a low level before the logarithmic growth phase. Expression levels reached a maximum at the 5th hour of the logarithmic phase, subsequently declined at the 6th hour, and remained at a low level thereafter (Lin *et al*., 2022). Furthermore, the copy number of *pirA* exhibited a significantly higher value in comparison to *pirB*, thereby confirming the results obtained from the experimental approach. These findings suggest that the mRNA expression level of *pirA* is significantly higher than that of *pirB* and thus

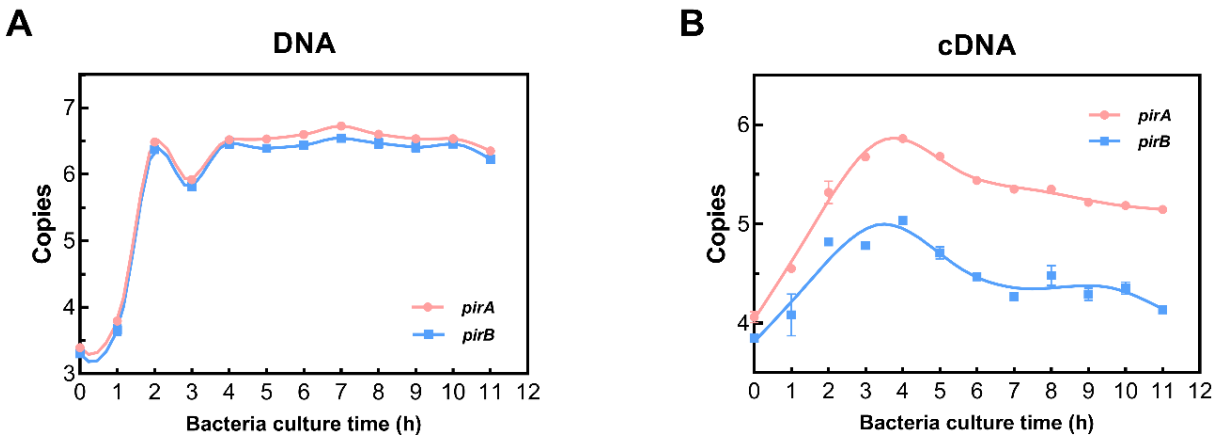


**Fig. 5** Determination of DNA content and mRNA expression levels of *pirA* (A) and *pirB* (B) at different growth stages of *V. parahaemolyticus* by qPCR. Error bars represent the mean ± SD (n = 3)

the transcription level of *pirA* consistently surpassed that of *pirB*. It is noteworthy that although the *pirA* and *pirB* genes are organized within a single operon in AHPND-causing *V. parahaemolyticus*, differential expression between the two genes was observed in our study. Such discrepancies have also been reported in other bacterial operons and may arise from differences in mRNA stability, transcript secondary structure, or translational efficiency, as well as from post-transcriptional regulatory mechanisms. These factors can lead to unequal accumulation of transcripts or proteins even under a shared promoter, which may explain the observed expression pattern of *pirA* and *pirB* in this work.

In the Dot Blot experiment, it was found that the protein expression levels of PirB were consistently significantly higher than those of PirA at different time points. This suggests that PirB may have a stronger expression advantage or translation efficiency at the translational level. However, these findings are in marked opposition to the results obtained at the transcriptional level. Consequently, we hypothesize that this is associated with post-transcriptional regulatory mechanisms, which are recognized as playing a pivotal role in gene expression control. The PirB protein may be more important in basal metabolism and requires sustained high expression, while PirA may be more needed at the transcriptional level, but its actual functional requirements may be adjusted through translational regulation. It has been reported that PirA and PirB toxins interact synergistically, exhibiting comparable toxicity to brine shrimp larvae, with PirB demonstrating a greater degree of toxicity than PirA (Kumar *et al*., 2019). Shrimp fed with PirB-specific VLRB antibodies exhibited significantly higher survival rates than those in the PirA group (Lazarte *et al*., 2021). Furthermore, the results of the report also showed that, the PirB toxin alone was capable of inducing the similar histological signs of AHPND when challenged by reverse gavage (Lee *et al*., 2015). A comparison of the performance of anti-PirA nanobodies and anti-PirB nanobodies revealed that the latter performed better in three areas: positive clone rate in phage ELISA, protein production, and antibody affinity. Furthermore, anti-PirB nanobodies exhibited higher sensitivity than anti-PirA nanobodies (Shao *et al*., 2025). Therefore, it can be inferred that the PirB protein is critical for the toxic function of AHPND and has higher expression levels, rendering it a priority target for the establishment of highly sensitive antibodies for rapid on-site detection.

In addition, experiments similar to those conducted with *V. parahaemolyticus* were performed using tissue samples from shrimp infected with AHPND, with the template being modified from bacteria to the hepatopancreas of infected shrimp. The results demonstrated that the copy numbers of the *pirA* and *pirB* genes in the DNA of diseased shrimp were essentially consistent, while the cDNA copy number of *pirA* was notably higher than that of *pirB*, which was aligned with the results from bacterial samples. Meanwhile, total protein was extracted from the samples of the hepatopancreas of infected shrimp for Dot Blot analysis, but no PirA or PirB proteins were detected. This may be attributable to low in vivo expression levels below the detection limit, rapid degradation of these proteins within host tissues, or the relatively low sensitivity of the Dot Blot assay. Previous studies have indicated that the detection sensitivity in infected tissue samples is lower than in pure bacterial cultures (Kongrueng *et al*., 2015). Previous reports showed that the limited sensitivity of the antibody-based strip was about 1000 times less than PCR (Wangman *et al*., 2020). Consequently, antibody-based protein detection in infected tissues is generally less sensitive than molecular methods like PCR. However, the Dot Blot assay was chosen for its simplicity and suitability for rapid screening in field or resource-limited settings, providing a cost-effective way to detect toxin proteins despite its lower sensitivity compared to ELISA or PCR.

Moreover, Dot Blot analysis was applied as a rapid screening approach for PirA and PirB proteins in prawn samples, particularly in the context of complex tissue extracts. Unlike Western Blot, Dot Blot does not require electrophoretic separation,

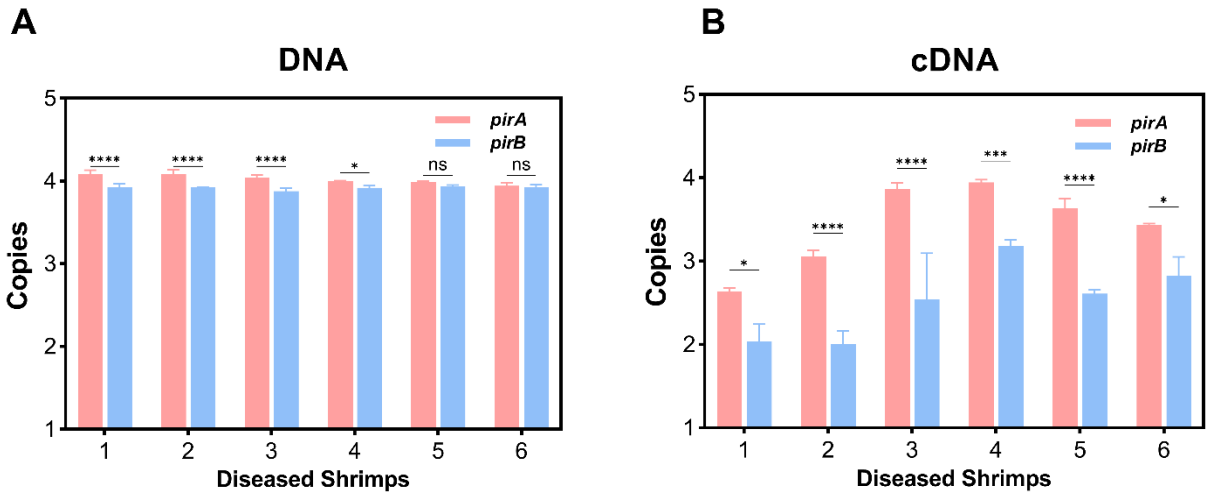


**Fig. 6** Determination of DNA content (A) and mRNA expression levels (B) of *pirA* and *pirB* in infected shrimp tissues with AHPND by qPCR. Error bars represent the mean ± SD of three technical replicates (n=3). Statistical analysis was performed using paired *t*-test where appropriate

which helps reduce potential antigen degradation or signal loss during sample processing. Given that one of the aims of this study was to verify toxin production at the protein level rather than to characterize precise molecular weights, Dot Blot analysis therefore represents a practical and complementary approach for AHPND-associated toxin detection within the scope of the present study. Future studies will incorporate more sensitive quantitative methods to further confirm these findings.

The research results presented here demonstrate that the nucleic acid and protein detection results of the pathogenic factors of AHPND are contradictory, thus suggesting that it may be inaccurate to rely on a solitary indicator for pathogen detection. In the process of disease diagnosis, while the detection of AHPND pathogenic genes is important, some studies have found that the virulence of *V. parahaemolyticus* depends on the expression of the PirA and PirB proteins rather than the copy number of the *pirA* and *pirB* genes (Tinwongger *et al*., 2016). Furthermore, it has been demonstrated that the partial deletion of the *pirA* or *pirB* gene, or the presence of the full-length gene without virulence protein expression, can result in a positive PCR outcome, despite the fact that PirA or PirB protein is not expressed (Han *et al*., 2017, Kanrar *et al*., 2018, Vicente *et al*., 2020). Accordingly, if the pathogen load is determined exclusively by nucleic acid testing, samples carrying plasmids but not expressing toxin proteins may be misinterpreted as diseased, resulting in false positives. Consequently, a solitary testing dimension is incapable of accurately reflecting the true disease status of the pathogen.

In summary, this study investigated the expression patterns and corresponding relationships of the pathogenic factors *pirA* and *pirB* of AHPND at the DNA, RNA, and protein levels. The nucleic acid and protein detection results of the pathogenic factors in AHPND were found to be inconsistent, indicating that reliance on a single indicator for pathogen detection may be an inaccurate approach. This provides a theoretical basis for selecting pathogen detection methods for shrimp. In the future, the diagnosis of AHPND could consider the combined use of multiple detection methods, based on the molecular mechanisms regulating toxin expression and screen for the optimal targets for detection.

**Acknowledgements**

This research is supported by the Science and Technology Talent Innovation Project of Hainan Province (KJRC2025B14 and KJRC2023A02), and the Innovation Capacity Enhancement Project of Hebei Province (253A6701D).

**References**

Dangtip S, Sirikharin R, Sanguanrut P, Thitamadee S, Sritunyalucksana K, Taengchaiyaphum S, *et al*. AP4 method for two-tube nested PCR detection of AHPND isolates of *Vibrio parahaemolyticus*. Aquac. Rep. 2: 158-162, 2015.

Duong ND, Mai-Hoang TD, Nguyen-Phuoc KH, Do KYT, Nguyen NTT, Tran TL, *et al*. Monitoring the secreted profile of PirA$^{vp}$ and PirB$^{vp}$ toxins from *Vibrio parahaemolyticus* causing acute hepatopancreatic necrosis disease. Aquac Int. 31(3): 1677-1684, 2023.

Duong ND, Nguyen-Phuoc KH, Mai-Hoang TD, Do KYT, Huynh TB, Nguyen NTT, *et al*. Fabrication of lateral flow immunoassay strip for rapid detection of acute hepatopancreatic necrosis disease. 3 Biotech. 12(10), 2022.

Han JE, Tang KFJ, Aranguren LF, Piamsomboon P. Characterization and pathogenicity of acute hepatopancreatic necrosis disease natural mutants, *pir*AB$_{vp}$ (-) *V. parahaemolyticus*, and *pir*AB$_{vp}$ (+) *V. campbellii* strains. Aquaculture 470: 84-90, 2017.

Han JE, Tang KFJ, Pantoja CR, White BL, Lightner DV. qPCR assay for detecting and quantifying a virulence plasmid in acute hepatopancreatic necrosis disease (AHPND) due to pathogenic *Vibrio parahaemolyticus*. Aquaculture 442: 12-15, 2015.

Han JE, Tang KFJ, Tran LH, Lightner DV. *Photorhabdus* insect-related (Pir) toxin-like genes in a plasmid of *Vibrio parahaemolyticus*, the causative agent of acute hepatopancreatic necrosis disease (AHPND) of shrimp. Dis. Aquat. Org. 113(1): 33-40, 2015.

Kanrar S, Dhar AK. Complete Genome Sequence of a Novel Mutant Strain of Vibrio parahaemolyticus from Pacific White Shrimp (Penaeus vannamei). Genome Announc. 6(24): 10.1128/genomea.00497-00418, 2018.

Kongrueng J, Tansila N, Mitraparp-arthorn P, Nishibuchi M, Vora GJ, Vuddhakul V. LAMP assay to detect *Vibrio parahaemolyticus* causing acute hepatopancreatic necrosis disease in shrimp. Aquac. Int. 23(5): 1179-1188, 2015.

Kumar V, Nguyen DV, Baruah K, Bossier P. Probing the mechanism of $VP_{AHPND}$ extracellular proteins toxicity purified from *Vibrio parahaemolyticus* AHPND strain in germ-free *Artemia* test system. Aquaculture 504: 414-419, 2019.

Lazarte JMS, Kim YR, Lee JS, Chun JH, Kim SW, Jung JW, *et al*. Passive Immunization with Recombinant Antibody VLRB-PirAvp/PirBvp-Enriched Feeds against *Vibrio parahaemolyticus* Infection in *Litopenaeus vannamei* Shrimp. Vaccines 9(1): 55, 2021.

Lee CT, Chen IT, Yang YT, Ko TP, Huang YT, Huang JY, *et al*. The opportunistic marine pathogen *Vibrio parahaemolyticus* becomes virulent by acquiring a plasmid that expresses a deadly toxin. Proc. Natl. Acad. Sci. U.S.A. 112(34): 10798-10803, 2015.

Li CL, Lin N, Feng ZH, Lin MH, Guan BY, Chen KS, *et al*. CRISPR/Cas12a Based Rapid Molecular Detection of Acute Hepatopancreatic Necrosis Disease in Shrimp. Front. Vet. Sci. 8, 2022.

Li LZ, Meng HM, Gu D, Li Y, Jia MD. Molecular mechanisms of V*ibrio parahaemolyticus* pathogenesis. Microbiol. Res. 222: 43-51, 2019.

Lin S-J, Huang J-Y, Le P-T, Lee C-T, Chang C-C, Yang Y-Y, *et al*. Expression of the AHPND Toxins PirAvp and PirBvp Is Regulated by Components of the *Vibrio parahaemolyticus* Quorum Sensing (QS) System. Int. J. Mol. Sci. 23(5): 2889, 2022.

Mai HN, Cruz-Flores R, Dhar AK. Development of an indirect Enzyme Linked Immunoassay (iELISA) using monoclonal antibodies against *Photorhabdus* insect related toxins, $PirA^{Vp}$ and $PirB^{Vp}$ released from *Vibrio* spp. J. Microbiol. Methods. 176, 2020.

Phiwsaiya K, Charoensapsri W, Taengphu S, Dong HT, Sangsuriya P, Nguyen GTT, *et al*. A Natural *Vibrio parahaemolyticus* Δ $pirA^{Vp}pirB^{Vp+}$ Mutant Kills Shrimp but Produces neither $Pir^{Vp}$ Toxins nor Acute Hepatopancreatic Necrosis Disease Lesions. Appl. Environ. Microbiol. 83(16): e00680-00617, 2017.

Shao SR, Yang HR, Zeng QF, Hu JJ, Wang MQ. Generation and evaluation of nanobodies specific for pirA and pirB from *Vibrio parahaemolyticus* causing acute hepatopancreatic necrosis disease. Aquaculture 602, 2025.

Sirikharin R, Taengchaiyaphum S, Sanguanrut P, Chi TD, Mavichak R, Proespraiwong P, *et al*. Characterization and PCR Detection Of Binary, Pir-Like Toxins from *Vibrio parahaemolyticus* Isolates that Cause Acute Hepatopancreatic Necrosis Disease (AHPND) in Shrimp. Plos One 10(5), 2015.

Tinwongger S, Nochiri Y, Thawonsuwan J, Nozaki R, Kondo H, Awasthi SP, *et al*. Virulence of acute hepatopancreatic necrosis disease PirAB-like relies on secreted proteins not on gene copy number. J. Appl. Microbiol. 121(6): 1755-1765, 2016.

Vicente A, Taengphu S, Hung AL, Mora CM, Dong H, Senapin S. Detection of *Vibrio campbellii* and *V. parahaemolyticus* carrying full-length $pirAB^{Vp}$ but only *V. campbellii* produces $Pir^{Vp}$ toxins. Aquaculture 519, 2020.

Wangman P, Chaivisuthangkura P, Taengchaiyaphum S, Pengsuk C, Sithigorngul P, Longyant S. Development of a rapid immunochromatographic strip test for the detection of *Vibrio parahaemolyticus* toxin B that cause acute hepatopancreatic necrosis disease. J. Fish Dis. 43(2): 207-214, 2020.

Zhou QQ, Wang Y, Hu JJ, Bao ZM, Wang MQ. Development of a real-time enzymatic recombinase amplification assay (RT-ERA) and an ERA combined with lateral flow dipsticks (LFD) assay (ERA-LFD) for rapid detection of acute hepatopancreatic necrosis disease (AHPND) in shrimp *Penaeus vannamei*. Aquaculture 566, 2023.